Eur. Phys. J. D **5**, 291–299 (1999)

THE EUROPEAN PHYSICAL JOURNAL D
EDP Sciences

Squeezed two-mode lasers without and with inversion

X.-M. Hu[a] and J.-S. Peng

Department of Physics, Huazhong Normal University, Wuhan 430079, P.R. China

Received: 22 December 1997 / Revised: 25 March 1998 / Accepted: 9 September 1998

Abstract. On the basis of the nondegenerate Λ quantum-beat laser model, we introduce a coherent field which drives the transition between the upper lasing level and an auxiliary level. We demonstrate that such a four-level system can produce squeezed two-mode laser without and with inversion. When the laser is operated well above threshold, the intensity fluctuation in the average mode is reduced below the shot noise with an optimum Mandel parameter $Q = -1/2$. At the same time, the noises in the relative amplitude and the relative phase drop to their vaccum noise levels. Furthermore, regardless of inversion, noninversion, and transition between inversion and noninversion, the optimum Mandel Q parameter of $Q = -1/2$ is retained when the system operates well above threshold. A simple physical explanation of the squeezing mechanism for two-mode squeezing is given.

PACS. 42.50.Lc Quantum fluctuations, quantum noise, and quantum jumps – 42.50.Ar Photon statistics and coherence theory – 42.50.Dv Nonclassical field states; squeezed, antibunched, and sub-Poissonian states; operational definitions of the phase of the field; phase measurements

1 Introduction

Recently considerable effort has gone to the study of lasing without inversion. Many models have been proposed, and the conditions for the onset of lasing action have been examined [1–10]. Experimentally lasing without population inversion has been observed [11–17]. Atomic coherence associated with the light amplification may lead to unusual statistical properties in inversionless lasers. Agarwal [18] showed that lasers without inversion may have a narrower linewidth than that of conventional lasers. Gheri and Walls [19] and Manka, Keitel, *et al.* [20] found that squeezed light can be produced in an inversionless closed Λ system and in an open Λ system, respectively. The maximum squeezing is up to 50% below the shot noise limit. Amplitude squeezing which is more than 50% below the shot noise limit has also been found in a cyclic Λ-type Raman laser by Ritsch and Marte, and Zoller [21], and in a four level V-type cyclic laser by Zhu, Rubiera, and Xiao [22]. In these systems, the enhancement of squeezing is due to additional dynamical pumping [23]. Including the effects of the detunings of laser transition and pump transition [24] or utilizing the initial atomic coherence [25] one can enhance squeezing with a Mandel Q parameter close to -1.

The studies on the statistical properties of lasers without inversion mainly focus on the single-mode system. In this paper we show that squeezed two-mode laser can be produced from a closed four-level system (as shown in Fig. 1a). The optimum Mandel Q parameters of $Q = -1/2$ are found when the laser is operated well above threshold. On the other hand, because of absence of positive inversion, it seems that a laser without inversion produces squeezing more effectively than a laser with inversion does. In this paper we also show that lasers with and without inversion produce squeezed light as effectively as each other.

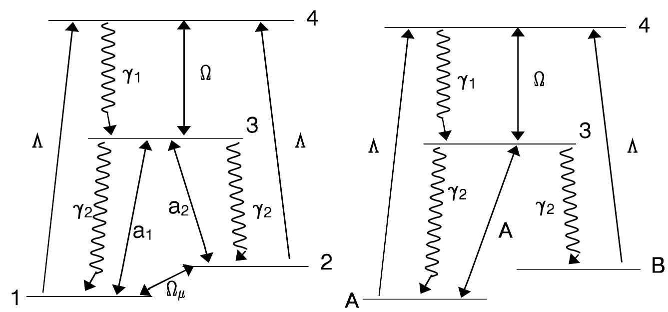

(a) (b)

Fig. 1. (a) Schematic representation of the four-level atom. (b) Atomic levels and transitions in the picture dressed by the microwave field.

In some recent papers there are some passive schemes which have been proposed to produce squeezed two-mode light, such as, multiwave mixing [26] and interaction of two-mode field with a cascade three-level atom [27]. Although good squeezing in one phase quadrature can be obtained, the squeezed light is very weak. The two-mode amplitude is much smaller than the spontaneous emission rates. As an active device of reducing noise, correlated

[a] e-mail: xmhu@ccnu.ml.org

spontaneous emission laser (CEL) has received considerable attention [28–34]. The CEL can be established by microwave coupling, initial atomic coherence, *etc.* Scully [28] first showed that, in V CEL, it is possible to eliminate the spontaneous emission fluctuations in the relative phase of the two laser modes. The prediction was verified by Winters, Hall and Toschek [31]. Two-mode two-photon CEL was found to produce two-mode squeezing [32]. The average phase and the relative amplitude exhibit 50% intracavity squeezing. However, only in the two-photon limit (*i.e.*, three-level two-mode two-photon CEL reduces to the effective two-level two-mode two-photon CEL [33]), is the squeezing significant. Here we show that the four-level system can produce bright squeezed laser light. The noise in the average amplitude is reduced 50% below the shot noise, and at the same time the noises in the relative amplitude and in the relative phase are reduced to vaccum noise levels.

The work is organized as follows. In Section 2 we present our model and derive the Langevin equations of the system. The quantum noises are calculated in Section 3. The main results are given in Section 4, respectively. A physical mechanism of squeezing and a summary are presented in Sections 5 and 6, respectively.

2 Model and equation

We consider a system of N closed four-level atoms as shown in Figure 1a. The energy level of the ith atomic level is $\hbar\omega_i$ ($i = 1$–4). The transitions $|1\rangle$–$|3\rangle$, $|2\rangle$–$|3\rangle$ and $|3\rangle$–$|4\rangle$ are dipole-allowed, and others are dipole-forbidden. $2\gamma_1$ and $2\gamma_2$ are the spontaneous decay rates, 2Λ is the incoherent pumping rate. For simplicity, we assume that the spontaneous decay rates from the level $|3\rangle$ to $|1\rangle$ and $|2\rangle$ are equal, and that the incoherent pumping rates from the levels $|1\rangle$ and $|2\rangle$ to the level $|4\rangle$ are equal. The double cavity resonantly contains the two lasing modes at frequencies ν_1 and ν_2. The two lasing modes are coupled to the transitions $|1\rangle$–$|3\rangle$ and $|2\rangle$–$|3\rangle$ *via* the coupling constants g_1 and g_2, respectively. The dipole transition $|3\rangle$–$|4\rangle$ is driven by a classical coherent field with frequency ν_3. This field will affect the atoms only through the Rabi frequency associated with it; it can thus be characterized by $\Omega(t) = \Omega\exp(-i\nu_3 t)$ where Ω denotes the Rabi frequency. The dipole-forbidden transition $|1\rangle$–$|2\rangle$ are strongly coupled by an external microwave of frequency ν and the corresponding Rabi frequency is $\Omega_\nu(t) = \Omega_\nu\exp(-i\phi)$ where Ω_ν and ϕ are the real amplitude and phase.

The Hamiltonian in the interaction picture for this system is [3,29]

$$V_{\rm I} = V_1 + V_2, \tag{1}$$

$$V_1 = -\sum_{\mu=1}^{N}\frac{1}{2}\hbar\Omega_\nu e^{i\phi}\sigma_{12}^\mu + H.c., \tag{2}$$

$$V_2 = \sum_{\mu=1}^{N}(i\hbar g_1 a_1^\dagger\sigma_{13}^\mu e^{-i\Delta_1 t} + i\hbar g_2 a_2^\dagger\sigma_{23}^\mu e^{-i\Delta_2 t} + i\hbar\Omega^*\sigma_{34}^\mu e^{-i\Delta_3 t}) + H.c., \tag{3}$$

where a_1, a_2 ($a_1^\dagger$, $a_2^\dagger$) are the annihilation (creation) operators for the two cavity fields, and $\sigma_{ij}^\mu = (|i\rangle\langle j|)^\mu$, ($i \neq j$, i, $j = 1$–4) are the atomic rasing or lowering operators. We have introduced the detunings as $\Delta_1 = \omega_3 - \omega_1 - \nu_1$, $\Delta_2 = \omega_3 - \omega_2 - \nu_2$, $\Delta_3 = \omega_4 - \omega_3 - \nu_3$, and assumed that the microwave field is resonant with the $|1\rangle$–$|2\rangle$ transition. Furthermore we assume $\Delta_1 = \Delta_2 = \Delta$ and $\Delta_3 = 0$.

Following standard techniques [35,36], we introduce dissipation by coupling the atoms and the two modes to reservoirs, and derive a master equation for the reduced-density operator ρ of the atoms and the two field modes. The resulting master equation in the interaction picture is

$$\frac{d\rho}{dt} = \frac{1}{i\hbar}[V_{\rm I},\ \rho] + \mathcal{L}_{a_1}\rho + \mathcal{L}_{a_2}\rho + \mathcal{L}_{34}\rho + \mathcal{L}_{13}\rho + \mathcal{L}_{23}\rho + \mathcal{L}_{14}\rho + \mathcal{L}_{24}\rho, \tag{4}$$

where

$$\mathcal{L}_{a_i}\rho = k(a_i\rho a_i^\dagger - a_i^\dagger a_i\rho - \rho a_i^\dagger a_i),\ i = 1,2,$$

$$\mathcal{L}_{34}\rho = \sum_{\mu=1}^{N}\gamma_1(\sigma_{34}^\mu\rho\sigma_{34}^{\dagger\mu} - \sigma_{34}^{\dagger\mu}\sigma_{34}^\mu\rho - \rho\sigma_{34}^{\dagger\mu}\sigma_{34}^\mu),$$

$$\mathcal{L}_{i3}\rho = \sum_{\mu=1}^{N}\gamma_2(\sigma_{i3}^\mu\rho\sigma_{i3}^{\dagger\mu} - \sigma_{i3}^{\dagger\mu}\sigma_{i3}^\mu\rho - \rho\sigma_{i3}^{\dagger\mu}\sigma_{i3}^\mu),\ i = 1,2,$$

$$\mathcal{L}_{i4}\rho = \sum_{\mu=1}^{N}\Lambda(\sigma_{i4}^{\dagger\mu}\rho\sigma_{i4}^\mu - \sigma_{i4}^\mu\sigma_{i4}^{\dagger\mu}\rho - \rho\sigma_{i4}^\mu\sigma_{i4}^{\dagger\mu}),\ i = 1,2.$$

For simplicity, we have assumed the equal cavity loss rates k for the two field modes.

We transform into the picture dressed by the microwave field (*i.e.*, the second interaction picture) [3,29], where V_1 is eliminated from the equation of motion, as

$$V_{\rm II} = e^{\frac{i}{\hbar}V_1 t}V_2 e^{-\frac{i}{\hbar}V_1 t}. \tag{5}$$

The following treatment is valid under the detuning condition which leads to correlated spontaneous emission [29], *i.e.*, $\Delta = \Omega_\nu/2$. Assuming $\Omega_\nu \gg \gamma_1, \gamma_2$ and Λ, we can introduce an effective rotating wave approximation (RWA) [3,29]. Then we can simplify the Hamiltonian in the second interaction picture. We define the sum and relative field operators for the two lasing modes as

$$A = (g_1 a_1 e^{-i\frac{\phi}{2}} + g_2 a_2 e^{i\frac{\phi}{2}})/\sqrt{2}G,$$
$$B = (g_2 a_1 e^{-i\frac{\phi}{2}} - g_1 a_2 e^{i\frac{\phi}{2}})/\sqrt{2}G, \tag{6}$$

in such a way that $[A, A^\dagger] = [B, B^\dagger] = 1$, $[A, B] = [A, B^\dagger] = 0$. One can now express a_1 and a_2 in terms of A and B. In equation (6) we have introduced the notation

$G = \sqrt{(g_1^2+g_2^2)/2}$. We also introduce the combination states for the atom

$$|A\rangle = \tfrac{1}{\sqrt{2}}(e^{i\frac{\phi}{2}}|1\rangle + e^{-i\frac{\phi}{2}}|2\rangle), \quad |B\rangle = \tfrac{1}{\sqrt{2}}(e^{i\frac{\phi}{2}}|1\rangle - e^{-i\frac{\phi}{2}}|2\rangle). \tag{7}$$

In the RWA, the interaction Hamiltonian reads as

$$V_{\rm II} = \sum_{\mu}^{N}(i\hbar G A^\dagger \sigma_{A3}^{\mu} + i\hbar\Omega_p^{*}\sigma_{34}^{\mu}) + H.c. \tag{8}$$

It is evident that the interaction Hamiltonian of the system is greatly simplified. It should be noted that the mode A is now resonantly coupled to the active laser media and the state $|B\rangle$ is decoupled from the interaction Hamiltonian. According to the simplified Hamiltonian we can plot the atomic levels and the transitions in Figure 1b. The driving transition $|3\rangle-|4\rangle$ remains unchanged and the transition $|3\rangle-|A\rangle$ represents lasing transition. In the second interaction picture the master equation (4) reduces to

$$\frac{d\rho}{dt} = \frac{1}{i\hbar}[V_{\rm II},\ \rho] + \mathcal{L}_A\rho + \mathcal{L}_B\rho + \mathcal{L}_{34}\rho + \mathcal{L}_{A3}\rho + \mathcal{L}_{B3}\rho + \mathcal{L}_{A4}\rho + \mathcal{L}_{B4}\rho, \tag{9}$$

where $\mathcal{L}_{34}\rho$ keeps unchanged. $\mathcal{L}_A\rho$, $\mathcal{L}_B\rho$, $\mathcal{L}_{A3}\rho$, $\mathcal{L}_{B3}\rho$, $\mathcal{L}_{A4}\rho$, and $\mathcal{L}_{B4}\rho$ have the same forms as $\mathcal{L}_{a_1}\rho$, $\mathcal{L}_{a_2}\rho$, $\mathcal{L}_{13}\rho$, $\mathcal{L}_{23}\rho$, $\mathcal{L}_{14}\rho$, and $\mathcal{L}_{24}\rho$ with the substitutions of A, B, σ_{A3}^{μ}, σ_{B3}^{μ}, σ_{A4}^{μ}, and σ_{B4}^{μ} for $a_1, a_2, \sigma_{13}^{\mu}$, σ_{23}^{μ}, σ_{14}^{μ}, and σ_{24}^{μ}, respectively.

We realize that there is no gain for the relative mode B (since the mode B is decoupled from the active atoms and the other mode A) and that the mode B is coupled to a loss reservoir (at zero temperature) only. Thus the relative mode B is always in its vaccum state. The matrix elements of the density operator for the mode B are

$$\rho_{n,m}^{(B)} = \delta_{n,m}\delta_{n,0}. \tag{10}$$

Since the relative mode B is in its vaccum state, the density operator ρ for the atoms and the mode A and B can be separated into two independent parts

$$\rho = \rho^{(A)}\rho^{(B)}, \tag{11}$$

where $\rho^{(A)}$ is the reduced density operator for the atoms and the mode A. Finally we obtain the master equation of reduced density operator $\rho^{(A)}$ of the atoms and the mode A

$$\frac{d\rho^{(A)}}{dt} = \frac{1}{i\hbar}[V_{\rm II},\ \rho^{(A)}] + \mathcal{L}_A\rho^{(A)} + \mathcal{L}_{34}\rho^{(A)} + \mathcal{L}_{A3}\rho^{(A)} + \mathcal{L}_{B3}\rho^{(A)} + \mathcal{L}_{A4}\rho^{(A)} + \mathcal{L}_{B4}\rho^{(A)}. \tag{12}$$

In order to determine the noise properties of the mode A, we apply a c-number Langevin approach. This operator master equation is equivalent to a c-number Fokker-Planck equation for the generalized P representation of Drummond and Gardiner [37]. We choose the normal ordering

$$A^\dagger, \sigma_{34}^{\dagger\mu}, \sigma_{A3}^{\dagger\mu}, \sigma_{A4}^{\dagger\mu}, \sigma_{B4}^{\dagger\mu}, \sigma_{B3}^{\dagger\mu}, \sigma_{BA}^{\dagger\mu}, \sigma_{4}^{\mu}, \sigma_{A}^{\mu}, \sigma_{B}^{\mu}, \sigma_{BA}^{\mu}, \sigma_{B3}^{\mu}, \sigma_{B4}^{\mu}, \sigma_{A4}^{\mu}, \sigma_{A3}^{\mu}, \sigma_{34}^{\mu}, A$$

where $\sigma_i^{\mu} = (|i\rangle\langle i|)^{\mu}$, $(i = A, B, 4)$ are the atomic population operators. We define a correspondence between c numbers and operators as

$$\alpha \leftrightarrow A, \quad v_1 \leftrightarrow \sum_{\mu=1}^{N}\sigma_{34}^{\mu}, \quad v_2 \leftrightarrow \sum_{\mu=1}^{N}\sigma_{A3}^{\mu}, \quad v_3 \leftrightarrow \sum_{\mu=1}^{N}\sigma_{A4}^{\mu}, \quad v_{Bi} \leftrightarrow \sum_{\mu=1}^{N}\sigma_{Bi}^{\mu}, \quad z_i \leftrightarrow \sum_{\mu=1}^{N}\sigma_{i}^{\mu},$$

$$\alpha^\dagger \leftrightarrow A^\dagger,\ v_1^\dagger \leftrightarrow \sum_{\mu=1}^{N}\sigma_{34}^{\dagger\mu}, \quad v_2^\dagger \leftrightarrow \sum_{\mu=1}^{N}\sigma_{A3}^{\dagger\mu}, \quad v_3^\dagger \leftrightarrow \sum_{\mu=1}^{N}\sigma_{A4}^{\dagger\mu},\ v_{Bi}^\dagger \leftrightarrow \sum_{\mu=1}^{N}\sigma_{Bi}^{\dagger\mu}.$$

We also adopt the following standard scaling of the variables and dipole coupling constant with the number of atoms as,

$$\alpha = \tilde{\alpha}N^{\frac{1}{2}}, \quad z_i = \tilde{z}_i N, \quad v_i = \tilde{v}_i N, \quad v_{Bi} = \tilde{v}_{Bi}N, \quad G = \tilde{G}N^{-\frac{1}{2}},$$

where a tilde denotes a scaled quantity. In the following we will drop the tilde for simplicity, keeping in mind that the c-numbers α, z_i, v_i, v_{Bi}, and G now denote the scaled quantities. Terms containing derivatives of higher than second order are negligible in the limit of many atoms. Finally we obtain the c-number Langevin equations of the mode A and atoms,

$$\dot{\alpha} = -k\alpha + Gv_2 + F_\alpha, \tag{13}$$
$$\dot{v}_1 = -\gamma_{34}v_1 + \Omega(z_4 - z_3) - G\alpha^\dagger v_3 + F_{v_1}, \tag{14}$$
$$\dot{v}_2 = -\gamma_{13}v_2 + G\alpha(z_3 - z_A) + \Omega^* v_3 + F_{v_2}, \tag{15}$$
$$\dot{v}_3 = -\gamma_{14}v_3 - \Omega v_2 + G\alpha v_1 + F_{v_3}, \tag{16}$$
$$\dot{v}_{Bi} = -\gamma_{Bi}v_{Bi} + F_{v_{Bi}},\ i = A, 3, 4, \tag{17}$$
$$\dot{z}_4 = -2\gamma_1 z_4 + 2\Lambda(z_A + z_B) - \Omega^* v_1 - \Omega v_1^\dagger + F_{z_4}, \tag{18}$$
$$\dot{z}_A = -2\Lambda z_A + 2\gamma_2 z_3 + G\alpha^\dagger v_2 + G\alpha v_2^\dagger + F_{z_A}, \tag{19}$$
$$\dot{z}_B = -2\Lambda z_B + 2\gamma_2 z_3 + F_{z_B}. \tag{20}$$

The closeness of the system requires $z_A + z_B + z_3 + z_4 = 1$. Here we only consider radiative decays. In equations (14–17) we have introduced $\gamma_{34} = \gamma_1 + 2\gamma_2$, $\gamma_{13} = \gamma_{B3} = \Lambda + 2\gamma_2$, $\gamma_{14} = \gamma_{B4} = \gamma_1 + \Lambda$, $\gamma_{BA} = 2\Lambda$.

We see from equation (17) that the polarizations v_{Bi} $(i = A, 3, 4)$ always are zero in the steady state and have no effect on the steady state laser intensities.

So among the atomic operators associated with the level $|B\rangle$, only the population operator σ_B contributes to the steady state laser intensities. We also see from equations (13–20) that v_{Bi} (i =A, 3, 4) are uncorrelated with the field operators and other atomic operators. As usual, we assume the atomic variables can be eliminated adiabatically. Under this condition, the noise in v_{Bi} is not coupled into the laser field mode A (also see Eqs. (22, 24, 26)). So, in the following we need not write out the noise correlations involved in the noise terms $F_{v_{Bi}}$. The other noise correlations are generally written as

$$\langle F_x(t)F_y(t')\rangle = 2\langle D_{xy}\rangle\delta(t-t'),$$

$$x,y=\alpha^\dagger, v_i^\dagger, z_j, v_i, \alpha;\quad i=1-3,\ j=A,B,4. \tag{21}$$

The nonzero diffusion coefficients $2\langle D_{xy}\rangle$ for the c-number variances are presented in Appendix A.

3 Calculation of noise

3.1 Mandel Q parameter for field mode A

After eliminating the atomic variables under the adiabatic elimination assumption, we obtain the Langevin equation for the photon number $I=\alpha^\dagger\alpha$ of the mode A as

$$\dot{I} = d_I + F_I. \tag{22}$$

The drift coefficient d_I and the Langevin force F_I are,

$$d_I = (G_{A3}-2k)I, \tag{23}$$

$$F_I = \alpha^\dagger F + \alpha F^\dagger, \tag{24}$$

where G_{A3} is the nonlinear gain, F is the Langevin force for the amplitude α,

$$G_{A3} = \frac{B_1 I_2 + C_1}{A I_2^2 + B_2 I_2 + C_2}, \tag{25}$$

$$F = F_\alpha + u_{11}F_{v_1} + u_{12}F_{v_2} + u_{13}F_{v_3} + u_{21}F_{v_1^\dagger} + u_{22}F_{v_2^\dagger} + u_{23}F_{v_3^\dagger} + u_{34}F_{z_4} + u_{3A}F_{z_A} + u_{3B}F_{z_B}. \tag{26}$$

In equations (25, 26) we have defined the laser intensity as $I_2 = G^2 I$. The parameters A, B_i, C_i and u_{ij} are presented in the Appendix B. The correlation for the intensity noise is written as

$$\langle F_I(t)F_I(t')\rangle = 2\langle D_{II}\rangle\delta(t-t'). \tag{27}$$

The expression for the diffusion coefficients $2\langle D_{II}\rangle$ is also presented in Appendix B.

Neglecting the noise F_I and setting the derivatives to zero in equation (22), we can obtain the laser intensity I_2 in the steady state. The steady state laser intensity I_2 above the lasing threshold is obtained as

$$I_2 = G^2 I = \frac{-B+\sqrt{B^2-4AC}}{2A}, \tag{28}$$

where

$$B = B_2 - \frac{B_1}{2k},\quad C = C_2 - \frac{C_1}{2k}.$$

The threshold condition is $C<0$, *i.e.*, $C_1/C_2 > 2k$. If the system operates well above threshold, we have $C_1/C_2 \gg 2k$.

The steady state atomic polarizations v_i and populations z_i, which are expressed in terms of the above laser intensity, are given in Appendix C.

The Mandel Q parameter in the steady state is obtained as,

$$Q = \frac{\langle(\Delta I)^2\rangle - I}{I} = \frac{\langle D_{II}\rangle}{\lambda I}, \tag{29}$$

where $\lambda = |\partial d_I(I)/\partial I|$ is the intensity fluctuation width. Q is a well-known measure of the deviation of the photon statistics from a Poissonian distribution ($Q=0$) which one finds for a coherent state. A negative Q (equivalent to sub-Poissonian statistics) is a signature of a nonclassical state of the field. The optimum Q parameter depends on λ. For $\lambda \ge 2k$, one has [23] $Q \ge -1/2$; for $\lambda \ge 4k$, however, one has [24,25] $Q \ge -1$.

The extracavity fluctuation spectrum $S(\omega)$ is related to the Q parameter through the following relation,

$$S(\omega) = 1 + 2Q\left(\frac{2k}{\lambda}\right)\frac{\lambda^2}{\lambda^2+\omega^2}, \tag{30}$$

where 1 is the shot noise. $S(\omega)=1$ corresponds to Poissonian statistics, $S(\omega)=0$ to perfect squeezing, and $0<S(\omega)<1$ to sub-Poissonian statistics. The output spectrum also depends on intensity fluctuation width λ. For $Q=-1/2$, when $\lambda=2k$ one has [23] $S(\omega)=0$, which corresponds to perfect squeezing, but when $\lambda=4k$, one has [19] $S(\omega)=1/2$, which corresponds to 50% squeezing.

3.2 Two-mode variance

In order to calculate the degree of two-mode squeezing, we first introduce Hermitian operators relating to the average amplitude B_R, the relative amplitude B_r, the average phase B_Θ, the relative phase B_θ, respectively ,

$$B_{R,r} = \frac{1}{\sqrt{8}}[(a_1e^{-i\phi/2} + a_1^\dagger e^{i\phi/2}) \pm (a_2 e^{i\phi/2} + a_2^\dagger e^{-i\phi/2})],$$

$$B_{\Theta,\theta} = \frac{-i}{\sqrt{8}}[(a_1e^{-i\phi/2} - a_1^\dagger e^{i\phi/2}) \pm (a_2 e^{i\phi/2} - a_2^\dagger e^{-i\phi/2})]. \tag{31}$$

In what follows, we assume $g_1=g_2=g$ and then have $G=g$. The modes A and B are written as

$$A = \frac{1}{\sqrt{2}}(a_1 e^{-i\frac{\phi}{2}} + a_2 e^{i\frac{\phi}{2}}),$$

$$B = \frac{1}{\sqrt{2}}(a_1 e^{-i\frac{\phi}{2}} - a_2 e^{i\frac{\phi}{2}}). \tag{32}$$

Expressing the a_1 and a_2 in terms of A and B, we have

$$\begin{aligned} B_R &= \mathrm{Re}(A/2), \\ B_r &= \mathrm{Re}(B/2), \\ B_\Theta &= \mathrm{Im}(A/2), \\ B_\theta &= \mathrm{Im}(B/2). \end{aligned} \tag{33}$$

The vaccum noise levels of all above operators are 1/4.

It is seen from equation (33) that the average amplitude operator B_R is identical to the amplitude operator $X = (A + A^\dagger)/2$ of the mode A. Therefore, the noise of the operator B_R equals the amplitude noise in the mode A, *i.e.*, $\langle(\Delta B_R)^2\rangle = \langle(\Delta X)^2\rangle$. When the steady state photon number I is far larger than unity (usually it is the case), the photon number variance of the mode A is related to $\langle(\Delta X)^2\rangle$ by the following relation [38]

$$\langle(\Delta I)^2\rangle = 4I\langle(\Delta X)^2\rangle. \tag{34}$$

It is easy to see from equation (29) that $\langle(\Delta X)^2\rangle$ is correlated to the Q parameter through the following relation

$$\langle(\Delta X)^2\rangle = \frac{1}{4}(1+Q). \tag{35}$$

If $Q = 0$, we have $\langle(\Delta X)^2\rangle = 1/4$, which corresponds to a two-mode coherent state with Poissonian statistics. If $Q < 0$, then $\langle(\Delta X)^2\rangle < 1/4$, which indicates occurrence of squeezing.

4 Results

4.1 Squeezing and lasing without inversion in the average mode

Here we first present the properties of the sum mode A. As the first step, let us consider the case where the lower lasing level is depleted and the coherent pumping to the upper level is strong, *i.e.*, Λ, $\Omega \gg \gamma_1, \gamma_2$. When the system operates well above threshold (*i.e.*, $C_1/C_2 \gg 2k$), the laser intensity is obtained as

$$I_2 = \sqrt{\frac{2G^2\Lambda I_1}{k}} \tag{36}$$

where $I_1 = \Omega^*\Omega$ is the intensity of the coherent driving field. For the usual good cavity case (*i.e.*, γ_1, $\gamma_2 \gg k$), one may have a large laser intensity, $I_2 \gg I_1$, Λ^2. At the moment, we obtain the population difference on the transitions $|3\rangle - |A\rangle$ as

$$z_3 - z_A = -\frac{I_1}{I_2}\,\cdot \tag{37}$$

It is seen that, in the microwave dressed picture, the mode A operates under noninversion. Then we can obtain the simple expressions for the intensity fluctuation width λ and the Mandel Q parameter as

$$\lambda = 4k + O\left(\frac{I_1^2}{I_2^2}\right), \tag{38}$$

$$Q = -\frac{1}{2} + O\left(\frac{I_1^2}{I_2^2}\right)\cdot \tag{39}$$

We see that the intensity fluctuation width $\lambda = 4k$ is twice much as the cavity loss rate $2k$ and the Q parameter is limited to $Q = -1/2$. That means that the intracavity field mode A exhibits maximal squeezing of 50%. It is seen from equation (30) that, $\lambda = 4k$ limits the output noise spectrum to $1 + Q$. The optimum value $Q = -1/2$ corresponds to 50% extracavity squeezing.

As the next step, we consider general cases *via* the numerical analysis. In Figures 2a and 2b we plot population difference $z_3 - z_A$, and Mandel Q parameter, respectively, *versus* the incoherent pumping rate Λ. It is easy to see that the mode A may not only operate without inversion for a large range of the parameters (as shown in (1) and (2) of Fig. 2a), but also exhibit transitions between inversion and noninversion (as shown in (3) and (4) of Fig. 2a). On the other hand, even though the system transits between noninversion and inversion, the laser intensity continues increasing (see the insert in Fig. 2b) and at the same time the Mandel Q parameter remains decreasing as the incoherent pumping rate Λ increases. Furthermore, when the incoherent pumping rate Λ is larger and thus the system operates well above threshold, the Mandel Q parameter approaches the optimum value $Q = -1/2$ (as shown in Fig. 2b). We can say that a laser with inversion produces squeezed light as effectively as a laser without inversion does.

In contrast to the passive schemes where good squeezing occurs only for weak fields [26,27], the present four-level system can produce bright squeezed laser light. Whether the system operates without or with inversion, the optimum Mandel Q parameter of $Q = -1/2$ can be achieved. This is one of the most important features of the four-level scheme.

4.2 Quenching of relative mode noise

Since the relative mode B is in its vaccum state, the noises in the relative amplitude and the relative phase drop to their vaccum noise levels,

$$\langle(\Delta B_{r,\theta})^2\rangle = \frac{1}{4}\,\cdot \tag{40}$$

That means the quenching of the spontaneous emission fluctuations in the relative amplitude and in the relative phase [28]. So, another feature of the four-level system is that, when 50% squeezing in the average amplitude is achieved, spontaneous emission fluctuations in the relative amplitude and in the relative phase are quenched.

4.3 Properties of each CEL mode a_1 and a_2

Furthermore, we show the statistical properties of each of the two modes a_1 and a_2. Since the mode B is in its vaccum state, according to the operator relations for the two

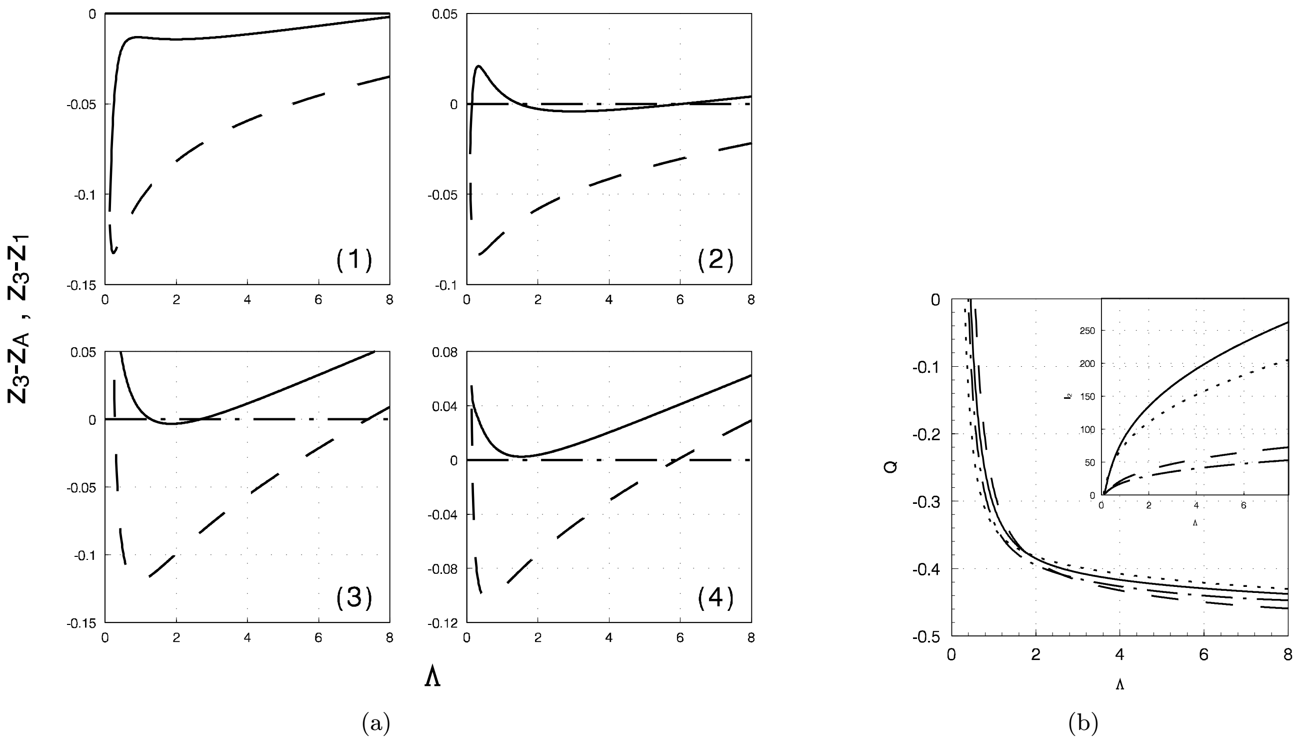

Fig. 2. (a) The population differences $z_3 - z_A$ (solid line) and $z_3 - z_1 (= z_3 - z_2)$ (dashed line) *versus* the incoherent pumping rate Λ. (1) corresponds to the parameters: $G = 1.0, k = 0.002, \gamma_1 = 0.1, \gamma_2 = 0.2, I_1 = 4.0$; (2) corresponds to the parameters: $G = 1.0, k = 0.01, \gamma_1 = \gamma_2 = 0.1, I_1 = 7.84$; (3) corresponds to the parameters: $G = 1.0, k = 0.002, \gamma_1 = \gamma_2 = 0.1, I_1 = 9.0$; (4) corresponds to the parameters: $G = 1.0, k = 0.01, \gamma_1 = \gamma_2 = 0.1, I_1 = 4.0$. (b) The Mandel Q parameter *versus* the incoherent pumping rate Λ. Solid, dashed, dotted, dotted-dashed lines correspond to the same parameters as in (1), (2), (3), (4) of (a), respectively. The insert shows the laser intensity I_2 *versus* the incoherent pumping rate Λ for the same parameters.

field modes (Eqs. (32)) we have the steady state photon numbers N_i $(i = 1, 2)$ of each of the two modes

$$N_1 = N_2 = \frac{1}{2} I. \tag{41}$$

Using the operator relations for the atomic combination states (Eqs. (7)), we easily obtain the population differences

$$z_3 - z_1 = z_3 - z_2 = z_3 - \frac{1}{2}(z_A + z_B). \tag{42}$$

The Mandel Q parameters for the two modes are [34]

$$Q_1 = Q_2 = \frac{1}{2} Q. \tag{43}$$

It is seen from equations (41–43) that the two CEL modes have the same properties. When Λ, $\Omega \gg \gamma_1$, γ_2 and $I_2 \gg \Lambda^2$, I_1, we easily find

$$z_3 - z_1 = z_3 - z_2 = -\frac{I_1}{I_2} \cdot \tag{44}$$

The system exhibits two-mode lasing without inversion in the bare atomic state. At the same time, the optimum Mandel Q parameter is $Q_1 = Q_2 = -1/4$. Therefore, we see that, when the system operates well above threshold, not only the mode A but also the two CEL modes operate without inversion and exhibit squeezing simultaneously.

For the general cases, we also plot in Figure 2a population difference $z_3 - z_1$ *versus* the incoherent pumping rate Λ. On one hand, the two CEL modes and the mode A can exhibit simultaneously lasing without inversion for a large range of parameters (as shown in (1–3) of Fig. 2a). On the other hand, we can see that the two CEL modes have a lot of different characteristics from the mode A. For example, the two CEL modes exhibit lasing with inversion when the mode A operates under noninversion (as shown in (4) of Fig. 2b). Especially, the two CEL modes exhibit transitions three times between inversion and noninversion while the mode A operates under noninversion (as shown in (2) of Fig. 2b). However, as the pumping rate Λ increases, the Q parameter tends to decreases. When the system operates well above threshold, the Mandel Q parameter approaches the optimum value $Q_1 = Q_2 = -1/4$ regardless of the transition between inversion and noninversion.

5 Discussion

Let us first compare the present scheme with the Λ schemes proposed by Gheri and Walls [19], Ritsch, Marte, and Zoller [21]. In their schemes, the auxiliary level is chosen such that no spontaneous emission from this level happens. The population in the upper lasing level is much smaller than the population in the lower lasing level. Thus one could expect that the spontaneous emission into the lasing mode is rather small compared to the standard laser. In the four-level system, however, the auxiliary level undergoes spontaneous emission. For convenience, we consider the mode A. Under the above conditions for the analytic solutions (Λ, $\Omega \gg \gamma_1$, γ_2), we have $z_4 \approx 1$. For the parameters for the above numerical solutions, we also have $z_4 \gg z_i$ ($i = A, B, 1, 2, 3$) when Λ is large; and at the same time, the population in the upper lasing level may be larger than the population in each of the lower lasing level (as shown in (3–4) in Fig. 2a). In spite of the above differences, the four-level system can produce the same squeezing as the Λ schemes do. It is evident that the squeezing does not depend on whether the system operates with inversion or without inversion.

In order to understand the physical picture of the two-mode squeezing, we consider the case where the lower lasing level is depleted and the coherent pumping to the upper level is strong, *i.e.*, Λ, $\Omega \gg \gamma_1$, γ_2. When the system operates well above threshold (*i.e.*, $C_1/C_2 \gg 2k$), the laser intensity is large, $I_2 \gg \Lambda^2$, I_1. Under these conditions we have $z_B \doteq 0$. Thus the present system (Fig. 1b) is reduced to a three-level system only with levels $|A\rangle$, $|3\rangle$ and $|4\rangle$. The transition $|A\rangle - |3\rangle$ is the lasing transition. The pumping process is a succession of the incoherent pump from level $|A\rangle$ to $|4\rangle$ and the coherent pump on the transition $|3\rangle - |4\rangle$. Such a succession of pumping processes recycles the active laser electron from the lower level $|A\rangle$ to the upper level $|3\rangle$ through level $|4\rangle$. It was shown [23] that the sequence of two incoherent steps leads to $Q = -1/4$. It is easy to understand that an incoherent step plus a coherent pump is more effective in noise reduction than the two incoherent steps. The succession of one incoherent step and a coherent driving leads to $Q = -1/2$. The large population in the auxiliary level $|4\rangle$ plays an important role in squeezing. As well-known, the coherent driving is always two-directional. However, when the population in level $|4\rangle$ is much larger than the population in level $|3\rangle$, the pump from level $|4\rangle$ to level $|3\rangle$ prevails over the pump from level $|3\rangle$ to level $|4\rangle$. As a result, the pump from level $|A\rangle$ to level $|3\rangle$ through $|4\rangle$ mainly is unidirectional. The unidirectional pump leads to regular recycling of the laser electron. Therefore, the physical picture of the noise suppression is that the succession of the incoherent and coherent processes leads to a regular recycling of the laser electron. In addition, the effects of the level $|B\rangle$ counteracts the squeezing because the recycling through the level $|B\rangle$ deviates the above recycling and so reduces the regularity of the laser electron. However, its influence is negligible so long as the Rabi frequency of the laser field is far larger than the decay rates,

Ideally, since the intensity fluctuation width $\lambda = 4k$ is twice large as the cavity loss rate $2k$, the Q parameter have an optimum value of -1. However, we only get $Q = -1/2$. This is because the mode A is resonant with the transition $|A\rangle - |3\rangle$. We might more easily understand this result in the picture dressed by the mode A. It should be noted that the mode A acts as a single mode. The strong laser field mode A leads to an ac-Stark splitting of the lasing transition, which is proportional to the Rabi frequency $G\alpha$. Due to the effects of the level shifts the coherent driving is detuned from the atomic dressed-state transition frequencies between states $|4\rangle$ and $|3\rangle$. For such a case, the cycling of the active laser electron is regularized moderately. On the basis of the above calculations and analyses, we can deduce that the depletion of the ground states and the strong coherent driving are the optimum conditions for squeezing. So we only have $Q = -1/2$. A possible example of a real atom for realization of the scheme could be found in neutral sodium. We identify the two components $F = 1$ and $F = 2$ of $3S_{1/2}$ as the ground level doublet $|1\rangle$ and $|2\rangle$, $3P_{1/2}$ as $|3\rangle$, and $4S_{1/2}$ as $|4\rangle$. Although there is an extra spontaneous emission channel from the level $|4\rangle$ through $|3\rangle$ to $|1\rangle$ and $|2\rangle$, its influence is negligible so long as the Rabi frequency of the driving field is far larger than the decay rates, just as the influence of the dressed-state level $|B\rangle$ is.

6 Conclusion

In summary, we have investigated the statistical properties of a four-level two-mode laser system. The main points are summarized as follows. The four-level system can produce squeezed two-mode laser without and with population inversion. Good squeezing is compatible with large laser intensity. When the two-mode laser is operated well above threshold, an optimum Mandel Q parameter of $Q = -1/2$ is obtained. At the same time, the relative amplitude and the relative phase exhibit the quenching of spontaneous emission fluctuations. Whether the system operates under inversion, or noninversion, or transition between inversion and noninversion, the optimum Mandel Q parameter of $Q = -1/2$ may be retained when the system operates well above threshold. Each CEL mode exhibits squeezing with the optimum Mandel Q parameter of $Q = -1/4$. Although the operation properties of the two CEL modes are similar to those of the sum mode A, there are a lot of differences between them. Especially, an interesting phenomenon is that, as the incoherent pumping rate increases, the two CEL modes transit three times between inversion and noninversion while the sum mode A operates under noninversion. Furthermore, a simple physical picture of squeezing mechanism is given. This mechanism is that the succession of incoherent pumping and the coherent driving leads to the regular recycling of the laser electron. Such an mechanism does not depend on whether the system operates with or without inversion. Therefore, the optimum squeezing is achieved both for inversion laser and for noninversion laser.

This work was supported by the National Natural Science Foundation of China and the Natural Science Foundation of Hubei Province.

Appendix A

The nonzero diffusion coefficients for the c-number variances are

$$\begin{aligned}
2\langle D_{v_1v_1}\rangle &= 2\Omega v_1,\\
2\langle D_{v_2v_2}\rangle &= 2G\alpha v_2,\\
2\langle D_{v_1^\dagger v_1}\rangle &= 4\gamma_2 z_4 + 2\Lambda(z_A+z_B),\\
2\langle D_{v_2^\dagger v_2}\rangle &= 2\Lambda z_3 + 2\gamma_1 z_4,\\
2\langle D_{v_3^\dagger v_3}\rangle &= 2\Lambda(z_4+z_A+z_B),\\
2\langle D_{v_2v_1}\rangle &= -\Omega v_2 + 4\gamma_2 v_1,\\
2\langle D_{v_3v_1}\rangle &= \Omega v_3,\\
2\langle D_{v_2^\dagger v_3}\rangle &= 2\Lambda v_1,\\
2\langle D_{z_4v_2}\rangle &= -2\Lambda v_2 + \Omega^* v_3,\\
2\langle D_{z_4v_3}\rangle &= -2\Lambda v_3,\\
2\langle D_{z_Av_1}\rangle &= -2\gamma_2 v_1,\\
2\langle D_{z_Av_2}\rangle &= 2\Lambda v_2,\\
2\langle D_{z_Av_3}\rangle &= 2\Lambda v_3,\\
2\langle D_{z_Bv_1}\rangle &= -2\gamma_2 v_1,\\
2\langle D_{z_4z_4}\rangle &= -\Omega v_1^\dagger - \Omega^* v_1 + 2\gamma_1 z_4 + 2\Lambda(z_A+z_B),\\
2\langle D_{z_Az_A}\rangle &= -G\alpha v_2^\dagger - G\alpha^\dagger v_2 + 2(\Lambda z_A + \gamma_2 z_3),\\
2\langle D_{z_Bz_B}\rangle &= 2\Lambda z_B + 2\gamma_2 z_3,\\
2\langle D_{z_4z_A}\rangle &= -2\Lambda z_A,\\
2\langle D_{z_4z_B}\rangle &= -2\Lambda z_B,\\
2\langle D_{v_1\alpha}\rangle &= -G v_3.
\end{aligned}$$

Appendix B

Here we list the parameters which appear in equation (25)

$$\begin{aligned}
A &= (T+1)\gamma_1 + \gamma_2 + \Lambda,\\
B_1 &= 2G^2\gamma_1(\Lambda-\gamma_2),\\
C_1 &= 2G^2\{[\Lambda(2\gamma_2-\gamma_1) + (\Lambda-\gamma_2)\gamma_{14}]I_1\\
&\quad + \gamma_1(\Lambda-\gamma_2)\gamma_{14}\gamma_{34}\},\\
B_2 &= [2\gamma_2-\gamma_1+(T+2)(\gamma_{14}-\Lambda)]I_1\\
&\quad + [\gamma_1(T\Lambda+\gamma_2)+2\Lambda\gamma_2]\gamma_{13} + [\Lambda+(T+1)\gamma_1+\gamma_2]\gamma_{14}\gamma_{34},\\
C_2 &= [(T+1)\Lambda+\gamma_2]I_1^2 + \{[\gamma_1(\gamma_2+T\Lambda)+2\Lambda\gamma_2)\gamma_{34}\\
&\quad + [(T+1)\Lambda+\gamma_2]\gamma_{14}\gamma_{13}\}I_1 + [\gamma_1(\gamma_2+T\Lambda)+2\Lambda\gamma_2]\gamma_{34}\gamma_{13}\gamma_{14}.
\end{aligned}$$

In the above expressions we have defined $T = 1 + \gamma_2/\Lambda$ and the intensity of the driving field $I_1 = \Omega^*\Omega$.

Then we present the parameters in equation (26)

$$\begin{aligned}
u_{11} &= G^2\alpha\Omega^*[U_1(\gamma_{14}\gamma_{13}+I_1) - U_2I_2 + 2]/2U\\
u_{12} &= G[U_1I_1I_2 + (2-U_2I_2)(\gamma_{14}\gamma_{34}+I_2)]/2U\\
u_{13} &= G\Omega^*[-(U_1\gamma_{13}+U_2\gamma_{34})I_2 + 2\gamma_{34}]/2U\\
u_{21} &= G^2\alpha\Omega[U_1(\gamma_{14}\gamma_{13}+I_1) - U_2I_2)]/2U\\
u_{22} &= G^3\alpha^2[U_1I_1 - U_2(\gamma_{14}\gamma_{34}+I_2)]/2U\\
u_{23} &= G^3\alpha^2\Omega(-U_1\gamma_{13} - U_2\gamma_{34})/2U\\
u_{34} &= -G^2\alpha U_1/2\\
u_{3A} &= -G^2\alpha U_2/2\\
u_{3B} &= -G^2\alpha(\frac{G_{A3}}{G^2\Lambda} + U_1)/2
\end{aligned}$$

with

$$\begin{aligned}
U &= \gamma_{34}\gamma_{13}\gamma_{14} + \gamma_{34}I_1 + \gamma_{13}I_2\\
U_1 &= [-(\gamma_2+T\Lambda+\Lambda)I_1 + (\Lambda-\gamma_2)I_2\\
&\quad + (\Lambda-\gamma_2)\gamma_{14}\gamma_{34}]/D\\
U_2 &= \{[(T+2)\gamma_{14}+\gamma_2-\gamma_1-(T+1)\Lambda]I_1\\
&\quad + [(T+1)\gamma_1+\gamma_2+\Lambda](I_2+\gamma_{14}\gamma_{34})\}/D.
\end{aligned}$$

Without loss of generality, in the steady state one can takes Ω, v_i, $(i = 1–3)$ and α to be real. Thus the diffusion coefficient $\langle D_{II}\rangle$ can be written as

$$\begin{aligned}
\langle D_{II}\rangle &= 2\sum_{i=1}^{3}(u_{1i}+u_{2i})^2(\langle D_{v_iv_i}\rangle + \langle D_{v_i^*v_i}\rangle)\\
&+ 4\sum_{i,j=1,i\neq j}^{3}(u_{1i}+u_{2i})(u_{1j}+u_{2j})(\langle D_{v_iv_j}\rangle + \langle D_{v_i^*v_j}\rangle)\\
&+ 8\sum_{i=A,B,4}\sum_{j=1}^{3}u_{3i}(u_{1j}+u_{2j})\langle D_{z_iv_j}\rangle + 4\sum_{i=A,B,4}u_{3i}^2\langle D_{z_iz_i}\rangle\\
&+ 8\sum_{i,j=A,B,4,i\neq j}u_{3i}u_{3j}\langle D_{z_iz_j}\rangle + 4(u_{21}+u_{11})\langle D_{v_1\alpha}\rangle.
\end{aligned}$$

Appendix C

The atomic polarizations and the atomic populations in the steady state are

$$\begin{aligned}
v_1 &= \Omega\Big\{\Lambda(2\gamma_2-\gamma_1)I_1 + [\gamma_1(\Lambda-\gamma_2)\\
&\quad + (\gamma_2+\Lambda-\gamma_1)\gamma_{14}]I_2 + \Lambda(2\gamma_2-\gamma_1)\gamma_{14}\gamma_{13}\Big\}/D\\
v_2 &= G\alpha\Big\{[\Lambda(2\gamma_2-\gamma_1) + \gamma_{14}(\Lambda-\gamma_2)]I_1\\
&\quad + \gamma_1(\Lambda-\gamma_2)I_2 + \gamma_1(\Lambda-\gamma_2)\gamma_{14}\gamma_{34}\Big\}/D
\end{aligned}$$

$$v_3 = \Omega G\alpha\Big[(\gamma_2 - \Lambda)I_1 + (\gamma_2 + \Lambda - \gamma_1)I_2 + \Lambda(2\gamma_2 - \gamma_1)\gamma_{13} + \gamma_1(\gamma_2 - \Lambda)\gamma_{34}\Big]/D$$

$$z_A = \Big\{\gamma_2 I_1^2 + \gamma_1 I_2^2 + (-\gamma_1 + \gamma_2 + \gamma_{14})I_1 I_2 + \gamma_2(\gamma_{14}\gamma_{13} + \gamma_1\gamma_{34})I_1 + \gamma_1(\gamma_{14}\gamma_{34} + \gamma_2\gamma_{13})I_2 + \gamma_1\gamma_2\gamma_{34}\gamma_{13}\gamma_{14}\Big\}/D$$

$$z_B = (T-1)z_3$$

$$z_3 = \Big\{\Lambda I_1^2 + \gamma_1 I_2^2 + (-\Lambda + \gamma_{14})I_1 I_2 + \Lambda(\gamma_{14}\gamma_{13} + \gamma_1\gamma_{34})I_1 + \gamma_1(\gamma_{14}\gamma_{34} + \Lambda\gamma_{13})I_2 + \Lambda\gamma_1\gamma_{34}\gamma_{13}\gamma_{14}\Big\}/D$$

$$z_4 = \Big\{\Lambda I_1^2 + (\gamma_2 + \Lambda)I_2^2 + (-2\Lambda + \gamma_2 + \gamma_{14})I_1 I_2 + \Lambda(\gamma_{14}\gamma_{13} + 2\gamma_2\gamma_{34})I_1 + [(\gamma_2 + \Lambda)\gamma_{14}\gamma_{34} + 2\Lambda\gamma_2\gamma_{13}]I_2 + 2\Lambda\gamma_2\gamma_{34}\gamma_{13}\gamma_{14}\Big\}/D$$

where

$$D = AI_2^2 + B_2 I_2 + C_2.$$

References

1. O. Kocharovskaya, Y.I. Khanin, Pis'ma Zh. Eksp. Teor. Fiz. **48**, 581 (1988); JETP Lett. **48**, 630 (1988).
2. S.E. Harris, Phys. Rev. Lett. **62**, 1033 (1989).
3. M.O. Scully, S.Y. Zhu, A. Garielides, Phys. Rev. Lett. **62**, 2813 (1989); E.E. Fill, M.O. Scully, S.Y. Zhu, Opt. Commun. **77**, 36 (1990).
4. A. Lyras, Z. Tang, P. Lambropoulos, J. Zhang, Phys. Rev. A **40**, 4131 (1989); S. Basile, P. Lambropoulos, Opt. Commun. **78**, 163 (1990).
5. O. Kocharovskaya, R.D. Li, P. Mandel, Opt. Commun. **77**, 215 (1990); O. Kocharovskaya, P. Mandel, *ibid.* **84**, 179 (1991); P. Mandel O. Kocharovskaya, Phys. Rev. A **46**, 2700 (1992).
6. A. Imamoglu, J.E. Field, S.E. Harris, Phys. Rev. Lett. **64**, 1154 (1991).
7. L.M. Narducci, H.M. Doss, P. Ru, M.O. Scully, S.Y. Zhu, C. Keitel, Opt. Commun. **81**, 379 (1991).
8. G.S. Agarwal, Phys. Rev. A **44**, R28 (1991), *ibid.* A **55**, 2467 (1997).
9. M.O. Scully, S.Y. Zhu, Z. Phys. **22**, 471 (1992); S. Y. Zhu, M.O. Scully, H. Fearn, L.M. Narducci, *ibid.* **22**, 483 (1992); H. Fearn, M.O. Scully, S.Y. Zhu, M. Sargent III, *ibid.* **22**, 495 (1992).
10. C.H. Keitel, O. Kocharovskaya, L.M. Narducci, M.O. Scully, S.Y. Zhu, Phys. Rev. A **48**, 3196 (1993).
11. J. Gao, C. Guo, X. Guo, G. Jin, P. Wang, J. Zhao, H. Zhang, Y. Jiang, D. Wang, D. Jiang, Opt. Commun. **93**, 323 (1992).
12. A. Nottelmann, C. Peters, W. Lange, Phys. Rev. Lett. **70**, 1783 (1993).
13. E.S. Fry, X. Li, D. Nikonov, G.G. Padmabandu, M.O. Scully, A.V. Smith, F.K. Tittel, C. Wang, S.R. Wilkinson, S.Y. Zhu, Phys. Rev. Lett. **70**, 3235 (1993).
14. W.E. van der Veer, R.J.J. van Diest, A. Donszelmann, H.B. van Linden van den Heuvell, Phys. Rev. Lett. **70**, 3243 (1993).
15. A.S. Zibrov, M.D. Lukin, D.E. Nikonov, L. Hollberg, M.O. Scully, V.L. Velichnsky, H.G. Robinson, Phys. Rev. Lett. **75**, 1499 (1995).
16. G.G. Padmabandu, G.R. Welch, I.N. Shubin, E.S. Fry, D.E. Nikonov, M.D. Lukin, M.O. Scully, Phys. Rev. Lett. **76**, 2053 (1996).
17. P.B. Sellin, G.A. Wilson, K.K. Weduri, T.W. Mossberg, Phys. Rev. A **54**, 2042 (1996).
18. G.S. Agarwal, Phys. Rev. Lett. **67**, 980 (1991).
19. K.M. Gheri, D.F. Walls, Phys. Rev. Lett. **68**, 3428 (1992); Phys. Rev. A **45**, 6675 (1992).
20. A.S. Manka, C.H. Keitel, S.Y. Zhu, M. Fleischhauer, L.M. Narducci, M.O. Scully, Opt. Commun. **94**, 174 (1992).
21. H. Ritsch, M.A.M. Marte, P. Zoller, Europhys. Lett. **19**, 7 (1993); H. Ritsch, M.A.M. Marte, Phys. Rev. A **47**, 2354 (1993).
22. Y. Zhu, M Xiao, Phys. Rev. A **48**, 3895 (1993).
23. H. Ritsch, P. Zoller, C.W. Gardiner, D.F. Walls, Phys. Rev. A **44**, 3361 (1991).
24. K.J. Schernthanner, H. Ritsch, Phys. Rev. A **49**, 4126 (1994).
25. C. Saavedra, J.C. Retamal, H. Keitel, Phys. Rev. A **55**, 3802 (1997).
26. B.A. Carpron, D.A. Holm, M. Sargent III, Phys. Rev. A **35**, 3388 (1987); S. An, M. Sargent III, Opt. Lett. **13**, 473 (1988); N.A. Ansari, M.S. Zubairy, Phys. Rev. A **38**, 2380 (1989).
27. J.P. Poizat, M.J. Collet, D.F. Walls, Phys. Rev. A **45**, 5171 (1992).
28. M.O. Scully, Phys. Rev. Lett. **55**, 2802 (1985).
29. M.O. Scully, M.S. Zubairy, Phys. Rev. **35**, 752 (1987); J.A. Bergou, M. Orszag, M.O. Scully, Phys. Rev. A **38**, 754 (1988).
30. W. Scheich, M.O. Scully, Phys. Rev. A **37**, 1261 (1988); W. Scheich, M.O. Scully, H.G. von Garssen, Phys. Rev. A **37**, 3010 (1988).
31. M.P. Winters, J.L. Hall, P.E. Toschek, Phys. Rev. Lett. **65**, 3116 (1990); I. Steiner, P.E. Toschek, Phys. Rev. Lett. **74**, 4639 (1995).
32. N. Lu, S.Y. Zhu, Phys. Rev. A **41**, 2865 (1990).
33. X.M. Hu, J.S. Peng, Acta Phys. Sin. **46**, 255 (1997) *(in Chinese)*.
34. N. Lu, Phys. Rev. A **45**, 8154 (1992).
35. H. Haken, in *Laser Theory*, edited by S. Flugge, Encyclopedia of Physics, Vol. XXV/2c (Springer-Verlag, Heidelberg, 1970).
36. W.H. Louisell, *Quantum Statistical Properties of Radiation* (Wiley, New York, 1973).
37. P.D. Drummond, C.W. Gardiner, J. Phys. A **13**, 2353 (1980).
38. R. Loudon, P.L. Knight, J. Mod. Opt. **34**, 709 (1987).